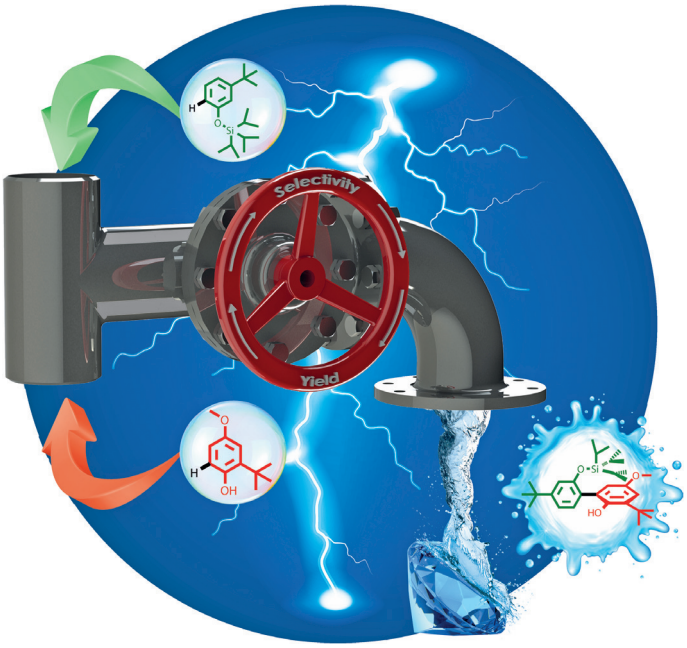

... leads to higher yield and selectivity in the electrochemical cross-coupling giving partially protected 2,2′-biphenols. In their Communication on page 11801 ff. S. Waldvogel and co-workers report the first direct synthesis of partially protected nonsymmetric biphenols by oxidative cross-coupling. The combination of the bulky triisopropylsilyl (TIPS) group and the solvent 1,1,1,3,3,3-hexafluoropropan-2-ol greatly broadens the scope of this sustainable synthesis.

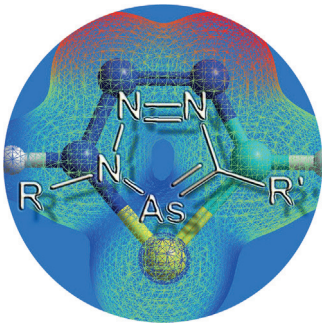

Arsenic Heterocycles

In their Communication on page 11760 ff. C. Müller et al. report a hitherto unknown triazaarsole. The synthesis was accomplished through a [3+2] cycloaddition reaction between an arsaalkyne and an organic azide.

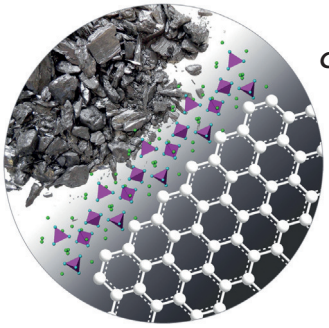

Graphene Oxide Synthesis

The synthesis of graphene oxide using ferrate(VI) ions has been proposed. In their Communication on page 11965 ff., Z. Sofer, M. Pumera, and co-workers show it is not possible owing to the fast decomposition of ferrate(VI).

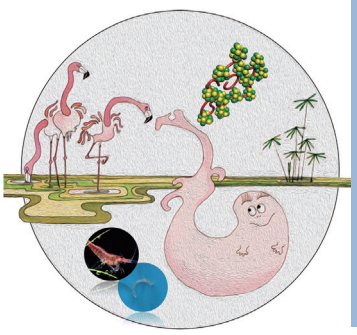

Mineral Plastics

In their Communication on page 11765 ff. H. Cölfen and co-workers report a plastic like bio-inspired hydrogel material that is shapeable and self-healable and can reversibly form rigid transparent films upon drying.

How to contact us:

Editorial Office:
E-mail: angewandte@wiley-vch.de
Fax: (+49) 62 01–606-331
Telephone: (+49) 62 01–606-315

Reprints, E-Prints, Posters, Calendars:
Carmen Leitner
E-mail: chem-reprints@wiley-vch.de
Fax: (+49) 62 01–606-331
Telephone: (+49) 62 01–606-327

Copyright Permission:
Bettina Loycke
E-mail: rights-and-licences@wiley-vch.de
Fax: (+49) 62 01–606-332
Telephone: (+49) 62 01–606-280

Online Open:
Margitta Schmitt
E-mail: angewandte@wiley-vch.de
Fax: (+49) 62 01–606-331
Telephone: (+49) 62 01–606-315

Subscriptions:
www.wileycustomerhelp.com
Fax: (+49) 62 01–606-184
Telephone: 0800 1800536 (Germany only)
+44(0) 1865476721 (all other countries)

Advertising:
Marion Schulz
E-mail: mschulz@wiley-vch.de
Fax: (+49) 62 01–606-550
Telephone: (+49) 62 01–606-565

Courier Services:
Boschstrasse 12, 69469 Weinheim

Regular Mail:
Postfach 101161, 69451 Weinheim

Angewandte Chemie International Edition is a journal of the Gesellschaft Deutscher Chemiker (GDCh), the largest chemistry-related scientific society in continental Europe. Information on the various activities and services of the GDCh, for example, cheaper subscription to *Angewandte Chemie International Edition*, as well as applications for membership can be found at **www.gdch.de** or can be requested from GDCh, Postfach 900440, D-60444 Frankfurt am Main, Germany.

GDCh
Gesellschaft Deutscher Chemiker

Service

Author Profile

"My favorite painter is M. C. Escher. I am waiting for the day when someone will discover teleportation. …"
This and more about Richard Hoogenboom can be found on page 11718.

News


C. A. Mirkin


A. P. Alivisatos


C. G. Hartinger


J. M. Thomas

Highlights

Antibiotics

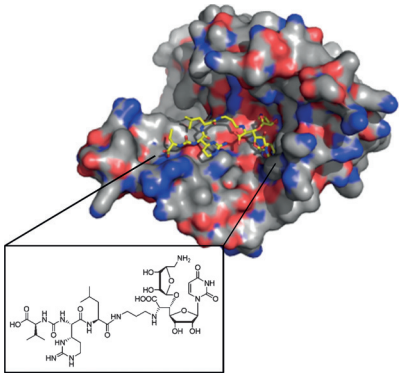

Natural(ly) fit: The X-ray crystal structure of the bacterial membrane protein MraY in complex with its natural product inhibitor muraymycin D2 is discussed. MraY catalyzes one of the membrane-associated steps in peptidoglycan biosynthesis and, therefore, represents a promising target for novel antibiotics. Structural insights derived from the protein–inhibitor complex might now pave the way for the development of new antimicrobial drugs.

Minireviews

Trifluoromethoxylation

One oxygen, three fluorines: Although the trifluoromethoxy group has very interesting properties, only few methods for its incorporation into organic compounds are currently available. This Minireview highlights some innovative and promising strategies that have recently emerged while demonstrating that further developments are necessary before a comprehensive "trifluoromethoxylation toolbox" is available.

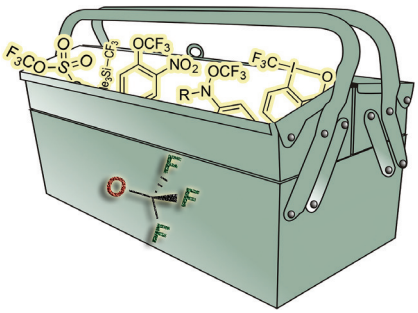

Reviews

Electrocatalysis

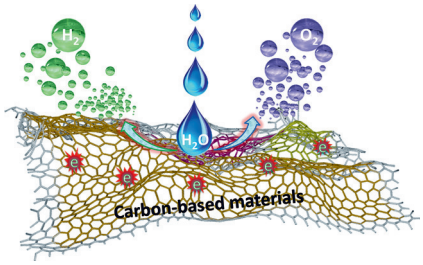

Free agents: Carbon-based metal-free catalysts have been intensively researched as alternatives to noble-metal/metal oxide catalysts for the oxygen evolution reaction (OER) in metal–air batteries and for the splitting of water through the hydrogen evolution reaction (HER). This Review gives an overview of recent developments in this area, with a focus on the OER and HER.

For the USA and Canada:
ANGEWANDTE CHEMIE International Edition (ISSN 1433-7851) is published weekly by Wiley-VCH, PO Box 101161, 69451 Weinheim, Germany. US mailing agent: SPP, PO Box 437, Emigsville, PA 17318. Periodicals postage paid at Emigsville, PA. US POSTMASTER: send address changes to *Angewandte Chemie*, John Wiley & Sons Inc., C/O The Sheridan Press, PO Box 465, Hanover, PA 17331. Annual subscription price for institutions: US$ 16.862/14.051 (valid for print and electronic / print or electronic delivery); for individuals who are personal members of a national chemical society prices are available on request. Postage and handling charges included. All prices are subject to local VAT/sales tax.

Communications

A facile route to a new class of arsenic heterocycles has been developed by making use of a [3+2] cycloaddition reaction between an arsaalkyne and an organic azide. The formation of the hitherto unknown air- and moisture-stable triazaarsole was verified by means of single-crystal X-ray diffraction (see picture; blue N). A comparison with triazaphospholes gives insight into the structural and electronic properties of this five-membered ring.

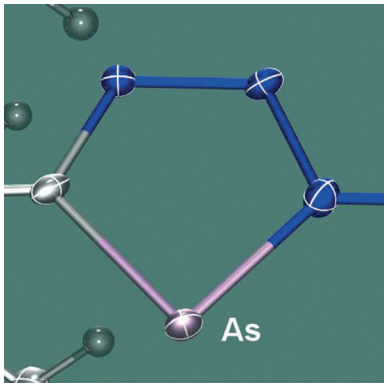

Arsenic Heterocycles

Shapeable, stretchable, recyclable, (thermochromic) amorphous calcium carbonate-based hybrid supramolecular hydrogels were synthesized, which can reversibly form macroscopic rigid transparent films upon drying. This plastic material may potentially replace conventional plastics in a move towards solving environmental issues.

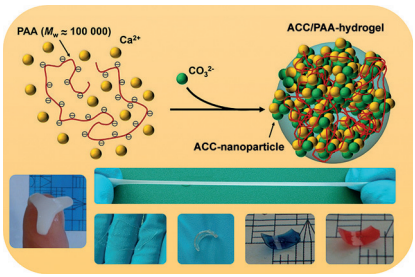

Plastics Substitutes

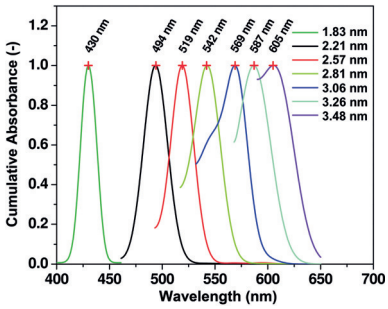

Size guide: nanoparticle sizes can be determined with sub-nm resolution, in solution without purification and fractionation. Using an analytical ultracentrifuge equipped with a newly developed multi-wavelength detector, simultaneous UV/Vis spectra are measured during the hydrodynamic separation of a mixture. The power of the method is demonstrated for the characterization of CdTe Nanoparticles.

Nanoparticle Analytics

Like in a molecular "Oscar" made of britannia-metal, Cu, Sn, and Sb atoms are combined in the heterometallic cluster anion $\{[CuSn_5Sb_3]^{2-}\}_2$ that was obtained by a reaction of $(Sn_2Sb_2)^{2-}$ with [nacnacCu(NCMe)]. It is shown by DFT calculations that as a result of the incorporation of the Cu atom, the monomeric units may be described as inhomogeneous superatoms, which are largely stabilized by dimerization—unlike isostructural and isoelectronic Sn_9^{2-}, which is a homogeneous superatom.

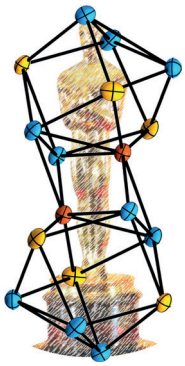

Cluster Compounds

Molecular Electronics

By varying the attachment points to the azulene center, the influence of the redox functionality on charge transport is evaluated. Among the three substituent patterns, only the 1,3 Az derivative displayed nonlinear and hysteretic transport behavior. Its weakly coupled LUMO is identified by DFT to be chargeable, leading to a transport mechanism also involving a slow electron-hopping channel, which is responsible for the switching due to single MO occupation.

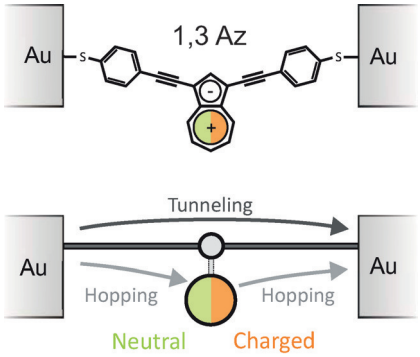

Chiral Ionic Liquids

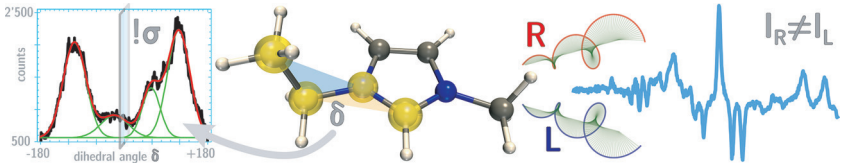

(A)chiral counterions: Chiral ionic liquids (CILs) are of increasing interest in asymmetric synthesis. In most CILs either the cation or the anion is chiral. Optical activity measurements show that, however, the symmetry of the achiral counterpart is broken in such environments, and thus chirality is induced. Therefore, also the achiral ions have to be carefully selected depending on the application of the chiral ionic liquid.

Antitumor Agents

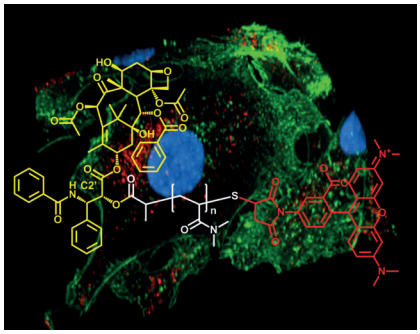

Visible effects: Well-defined paclitaxel–polymer conjugates with high drug loading, water solubility, and stability were obtained by a grafting-from approach. They are readily taken up into endosomes where native paclitaxel is efficiently released. The versatility of this approach was further demonstrated by post-functionalization with a fluorescent tracer.

Epigenetics

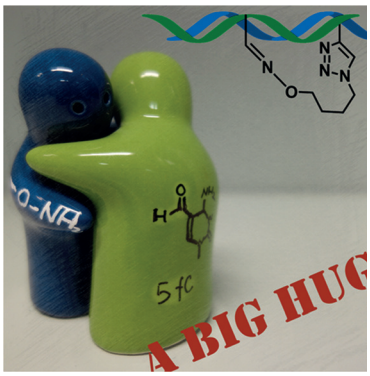

Big hug for fdC: A method for the site-specific quantification of the epigenetic base 5-formylcytosine (fdC) was developed. Applied on the genome of an mESC population, the assay showed that the repair enzyme Tdg removes only half of the fdC bases at a given genomic site.

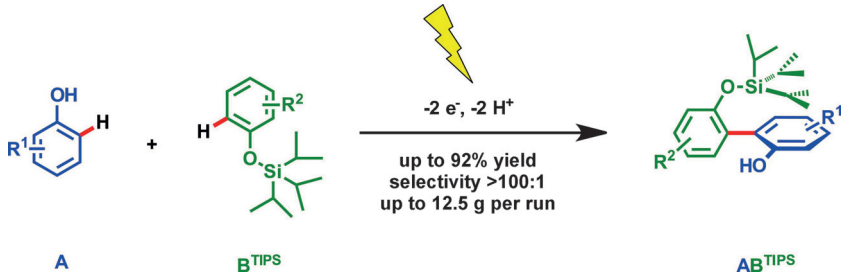

Twisted for success: The anodic cross-coupling of partially protected 2,2′-biphenols has been achieved with high yield and excellent selectivity. The combination of the bulky triisopropylsilyl (TIPS) group and the solvent 1,1,1,3,3,3-hexafluoropropan-2-ol greatly broadens the scope of this sustainable synthesis.

2,2′-Biphenols

Front Cover

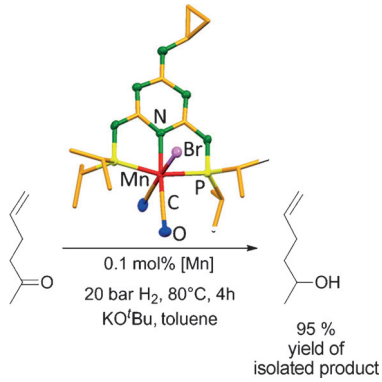

Manganese, if you please: An efficient and selective PN_5P-ligand-stabilized manganese C=O bond hydrogenation catalyst is able to quantitatively hydrogenate various diaryl, aryl–alkyl, dialkyl, and cycloalkyl ketones with catalyst loadings as low as 0.1 mol%. Additionally, various functional groups are tolerated, including unsubstituted olefins.

Hydrogenation Catalysts

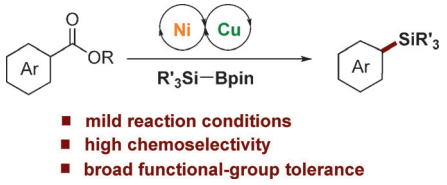

Copper and nickel: An efficient nickel/copper-catalyzed decarbonylative silylation reaction of carboxylic acid esters with silylboranes is described. This process provides access to structurally diverse aryl- and heteroarylsilanes directly from the corresponding esters and benefits from superior functional-group tolerance.

Cross-Couplings

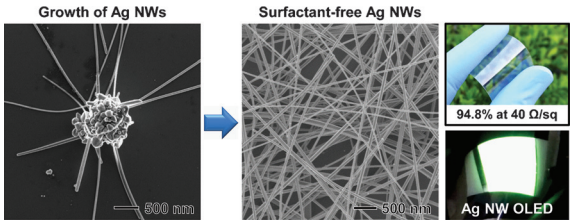

Stable without a stabilizer: Silver nanowires (NWs) were produced by polyol reduction in high yield without an organic stabilizer. Trace amounts of NaCl and $Fe(NO_3)_3$ enabled the heterogeneous nucleation and growth of Ag NWs on initially formed AgCl particles (see picture), and unwanted Ag nanoparticles were removed by oxidative etching. The resulting long NWs could be used directly for the fabrication of transparent or highly stretchable electrodes.

Nanotechnology

Charge-Transfer Interfaces

The surface of WO_3 photoanodes is dramatically activated after in situ formation of an overlayer with dual tungsten and oxygen vacancies, presenting a photocurrent density of 2.81 mA cm^{-2} at 1.23 V (vs. RHE) and a negative shift of the onset potential.

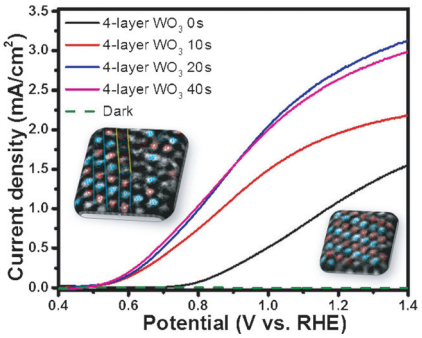

Indole Synthesis

All of me(so): A ruthenium-catalyzed [2+2+1+1] cycloaddition provided a common *meso*-hydroquinone intermediate for formal syntheses of the indole alkaloids *cis*-trikentrin A and herbindole B (see scheme). Key steps of the synthesis include a sterically demanding Buchwald–Hartwig amination and an unprecedented C(sp^3)–H amination/indolization reaction.

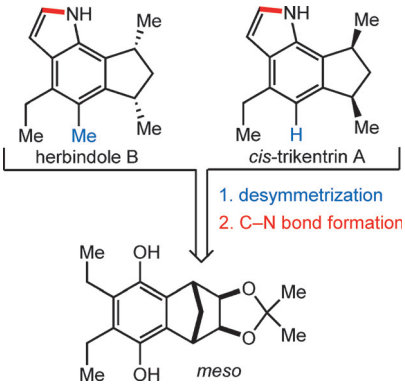

Phosphorus Nanowires

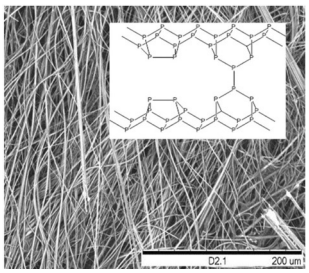

Red, red wire: The heating of amorphous red phosphorus powder and a thin film of red phosphorus film on a silicon wafer in a sealed ampoule resulted in a mm-long, uniform, and dense phosphorus nanowire network. Field effect transistor (FET) devices constructed with the red phosphorus nanowires displayed similar properties black phosphorus. A significant response to infrared light was observed from the FET device.

Asymmetric Catalysis

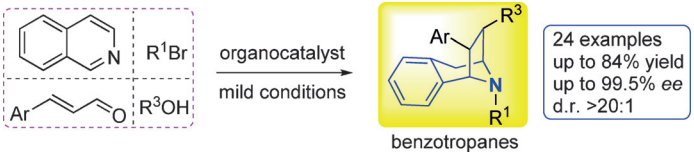

Fab four: A highly stereoselective dearomatizing double Mannich reaction of readily available isoquinolines, which provided two reactive sites for dearomatization, smoothly produced substituted benzotropanes with four contiguous stereocenters. In particular as a four-component reaction, this transformation shows high potential for the efficient diversity-oriented synthesis of useful tropane derivatives (see scheme).

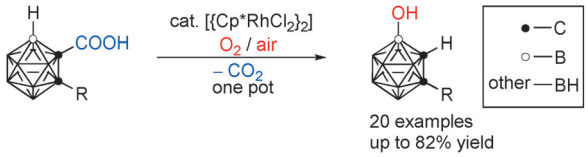

Cage decorations: The title reaction of a cage B4–H bond in *o*-carboranes with either O_2 or air as the oxygen source serves as a new method for the regioselective generation of a series of 4-OH-*o*-carboranes in a one-pot process. The use of either O_2 or air as both the oxidant and the oxygen source makes this protocol environmentally friendly and practical. Cp* = C_5Me_5.

B–H Activation

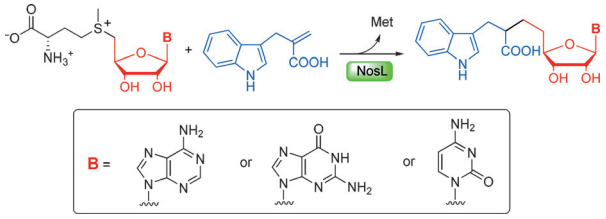

SAM switch-up: The SAM-dependent enzyme NosL was shown to switch from hydrogen abstraction to radical addition reaction when using an olefin-containing substrate analogue. Two SAM analogues with different nucleosides are able to initiate the radical-based reactions comparable to SAM, offering a way to expand SAM-dependent reactions and access new nucleoside-containing compounds.

Bioorganic Radicals

Pyridinic-N-tuned catalysis: An electron-rich pyridinic-N dopant modulates the electronic interactions between the active sites of palladium nanoparticles and the carbon support. Formic acid dehydrogenation at room temperature is significantly boosted by the pyridinic-N-doped palladium catalyst, presenting an efficient and reliable route to clean H_2 generation and sustainable energy storage.

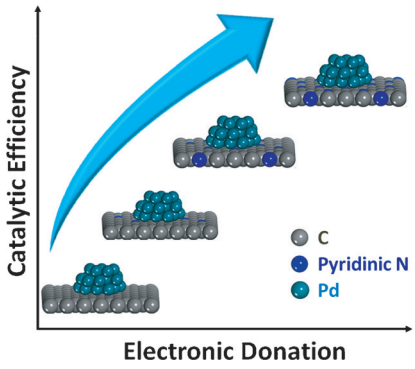

Hydrogen Storage Materials

A lead-free semiconducting hybrid ferroelectric, consisting of a zero-dimensional perovskite-like structure, exhibits large ferroelectric polarizations and notable semiconducting properties. The perovskite-derived framework dictates charge transport, while the organic cation determines ferroelectric behavior.

Ferroelectric Materials

Asymmetric Catalysis

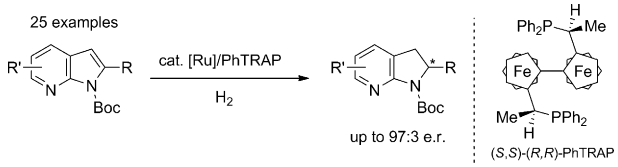

Caught in a TRAP: Chemo- and enantioselective hydrogenation of azaindoles were achieved, affording optically active 7-, 6-, 5-, and 4-azaindolines with up to 97:3 e.r. This reaction was catalyzed by a chiral ruthenium catalyst derived from [Ru(η³-methallyl)$_2$(cod)] and the *trans*-chelating chiral bis(phosphine) ligand, PhTRAP. Treatment of the reduction products with Pt/C under hydrogen gave the corresponding octahydroazaindoles with all-*cis* stereochemistry.

Oxygen Heterocycles

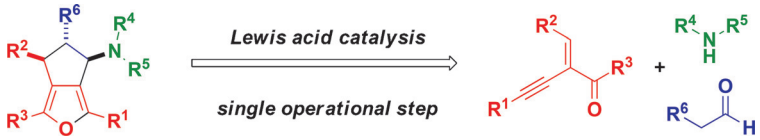

A diastereoselective three-component reaction between alkynyl enones, aldehydes and secondary amines is reported. With the aid of a benign indium catalyst, a range of highly substituted cyclopenta[*c*]furan derivatives is obtained in a single-step procedure. The formation of the stereodefined heterocyclic motifs takes place through in situ generation of an enamine followed by two sequential cyclization steps.

Heterocycles

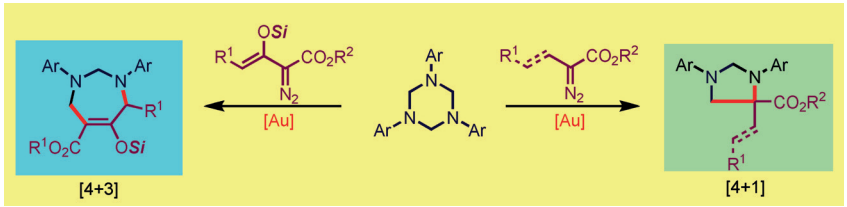

Golden performance: The title reaction has been accomplished, thus providing five- and seven-membered heterocycles in moderate to high yields under mild reaction conditions. These reactions feature the use of a gold complex to accomplish the diverse annulations and serve as an example of the involvement of a gold metallo-enolcarbene in a cycloaddition. *Si* = silyl protecting group.

Biomass

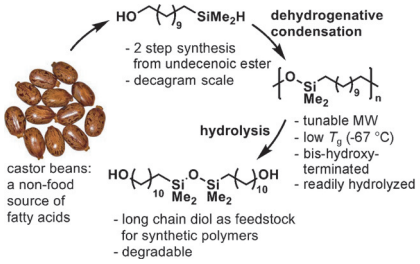

Cradle to grave: Castor oil derivatives were converted into polysilylethers (PSEs) by step-growth polymerization. The hydrolytically labile silyl ether linkages allowed facile degradation of the polymers into a degradable diol, thus completing the life cycle of the polymer. The PSEs possess a low glass-transition temperature (T_g), tunable molecular weight, and two hydroxy termini, which enable the construction of polyurethanes from the PSEs.

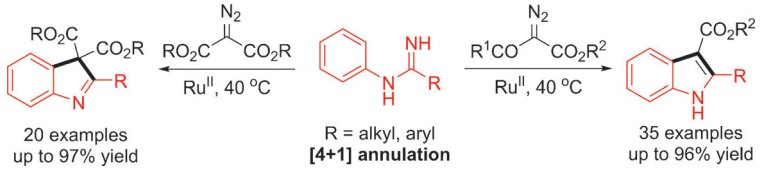

Which way to go: NH indoles and 3*H*-indoles were synthesized by ruthenium(II)-catalyzed C–H activation of imidamides and intermolecular coupling with diazo compounds under mild conditions. The coupling of α-diazoketoesters afforded NH indoles by cleavage of the $C(N_2)$–C(acyl) bond whereas α-diazomalonates gave 3*H*-indoles by C=N bond cleavage.

C–H Activation

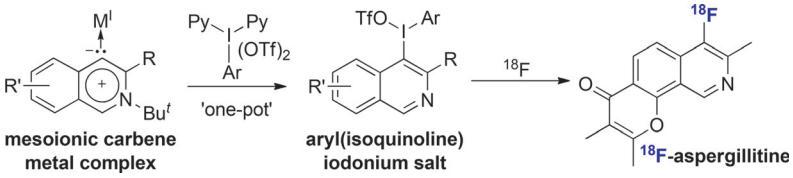

An efficient one-pot method to assemble aryl(isoquinoline)iodonium salts has been developed from mesoionic carbene silver complex and $ArylIPy_2(OTf)_2$. The process is compatible with well-functionalized molecules and was utilized for the preparation of ^{18}F-labeled isoquinolines in up to 92% radiochemical yield (RCY). As proof of concept, a fluorinated isoquinoline alkaloid, ^{18}F-aspergillitine was prepared in 10% RCY.

Radiofluorination

A rigid-tether strategy is developed to regioselectively synthesize the labile 1,2,3,4-bis(triazolino)[60]fullerene. Subsequent thermolysis treatment gives rise to several unprecedented structures (see picture), which were all characterized with single-crystal X-ray crystallography, providing concrete evidence for the formation mechanism of [60]bis-azafulleroids to clarify the long-term confusion.

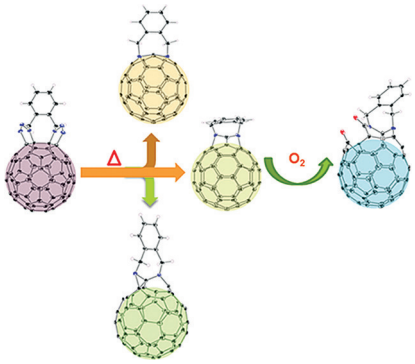

Fullerenes

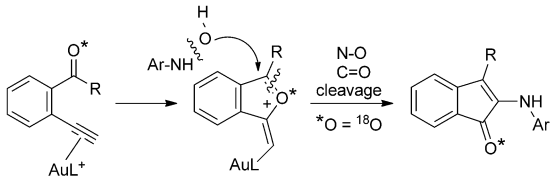

Under attack: The title reaction efficiently yields 2-aminoindenone derivatives. Experimental data suggests that this process involves an α-oxo gold carbene intermediate, generated from the attack of N-hydroxyaniline on a furylgold carbene intermediate, rather than the typical attack of oxidants on π-alkynes.

Heterocycle Synthesis

Amidation Reactions

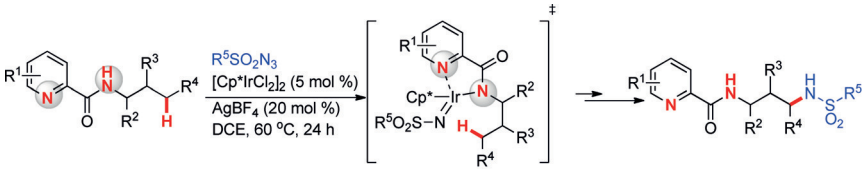

Regioselective intermolecular sulfonylamidation of unactivated secondary $C(sp^3)$–H bonds has been achieved using Ir^{III} catalysts. N,N′-bichelating ligand plays a crucial role in enabling iridium nitrene insertion into secondary $C(sp^3)$–H bonds via an outer-sphere pathway. This method tolerates a broad range of linear and branched-chain *N*-alkylamides, and provides efficient access to diverse γ-sulfonamido-substituted aliphatic amines.

Hydrogen Peroxide Adducts

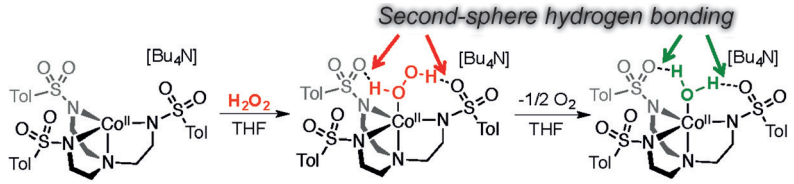

Finally confirmed: The first $M(H_2O_2)$ adduct with a redox-active metal, cobalt(II), could be directly detected in solution. This $Co^{II}(H_2O_2)$ compound is made observable by incorporating second-sphere hydrogen-bonding interactions between bound H_2O_2 and the supporting ligand, a trianionic trisulfonamido ligand. The decay kinetics and binding constant of this compound are discussed.

Balz–Schiemann Reaction

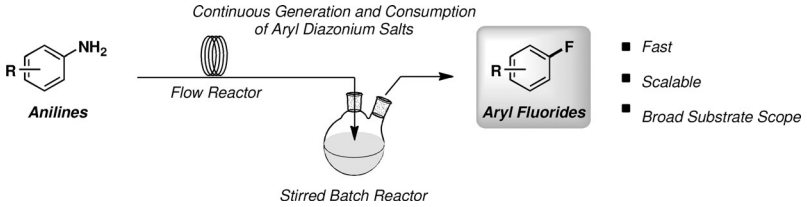

Go with the flow: A new continuous flow process for the Balz–Schiemann reaction has been developed. This process obviates the need to isolate potentially hazardous aryl diazonium salts. The short residence and collection times of the process enable the rapid preparation of aryl fluorides from anilines. This process tolerates a broad array of functional groups as well as both aryl and heteroaryl amines.

Multicomponent Reactions

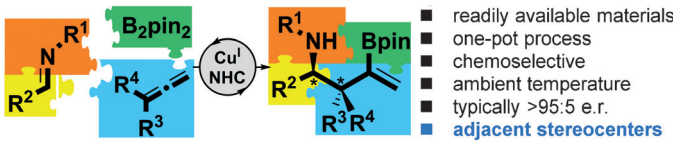

A copper-catalyzed three-component coupling affords homoallylic amines with adjacent stereocenters from achiral starting materials with high enantio- and diastereoselectivity. The method utilizes a commercially available NHC ligand and copper source, operates at ambient temperature, couples simple imines, allenes, and diboranes, and yields valuable homoallylic amines with versatile amino, alkenyl, and boryl units.

A new xenon(II) oxide: The Xe^{II} oxide cation, $[XeOXe]^{2+}$, has been synthesized at low-temperature as its CH_3CN adduct salt, $[CH_3CN{-}{-}{-}XeOXe{-}{-}{-}NCCH_3][AsF_6]_2$, and characterized by low-temperature single-crystal X-ray diffraction and Raman spectroscopy. Computational methods were used to assess the bonding in $[XeOXe]^{2+}$ and its adduct. The dication is the second example of a Xe^{II} oxide and is stabilized by CH_3CN through σ-hole type interactions.

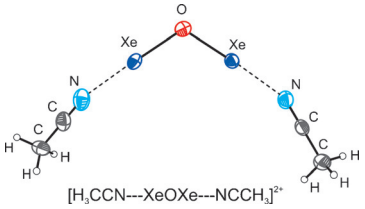

Noble-Gas Chemistry

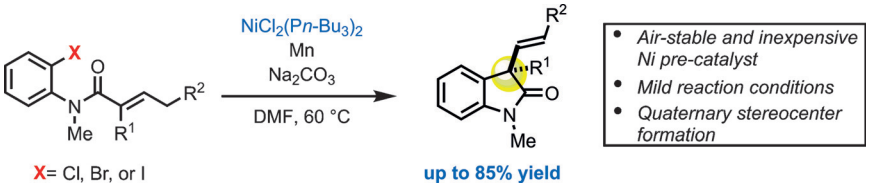

Affordable complexity: A nickel-catalyzed Heck cyclization for the construction of quaternary stereocenters was developed in the context of the synthesis of 3,3-disubstituted oxindoles (see scheme), which are prevalent motifs in biologically active molecules. The efficient reaction shows broad scope and provides a rare means to construct stereochemically complex frameworks by catalysis with nonprecious metals.

Synthetic Methods

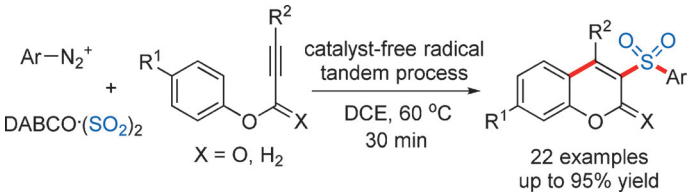

A dab of radicals: A catalyst-free approach enables the generation of sulfonyl radicals from aryldiazonium tetrafluoroborates in the presence of $DABCO{\cdot}(SO_2)_2$. The reaction affords 3-sulfonated coumarins in good to excellent yields. Additionally, the in situ diazotization of a number of anilines allows the directional synthesis of 3-sulfonated coumarins in a one-pot, two-step process. DABCO = 1,4-diazabicyclo-[2.2.2]octane.

Heterocycles

Good vibrations: Using vibrational spectroscopy and quantum mechanical calculations, the contrasting IR spectral features in the lowest triplet and ground states provide new experimental evidence for aromaticity reversal in [26]- and [28]hexaphyrins.

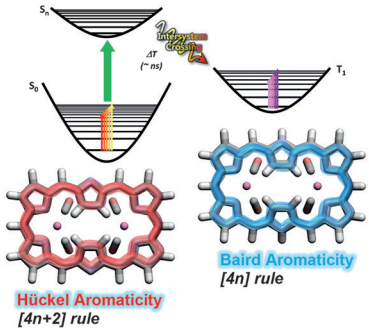

Aromaticity Reversal

Anticancer Agents

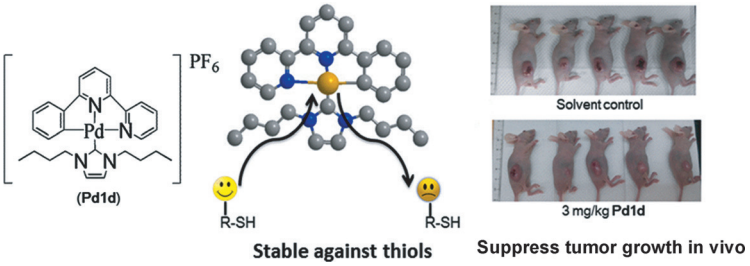

Stable antitumor agent: $[Pd(C^N^N)(NHC)]^+$ complexes demonstrate excellent stability in vitro and in aqueous solutions containing physiological thiols. This may allow the complexes to show potent in vitro cytotoxicity against cancer cells and in vitro angiogenesis at subcytotoxic concentrations, as well as effective in vivo anticancer activities toward tumor xenografts in nude mice with no observable toxicity.

Molecular Bioenergetics

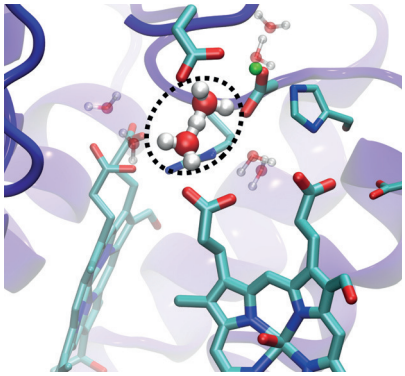

Proton-coupled electron transfer: Structurally conserved water molecules (see picture) function as a transient proton-loading site and provide important coupling elements in the proton-pumping machinery of cytochrome oxidase. Quantum mechanics/molecular mechanics simulations were used to study the biomolecular mechanism.

Optoelectronic Devices

A high-performance photodetector was realized by modification of a WSe_2 monolayer using a laser-healing technique and perovskite functionalization. Modification and interface engineering of transition-metal-dichalcogenides with halide perovskites, yields hybrid materials that may be promising building blocks in optoelectronics.

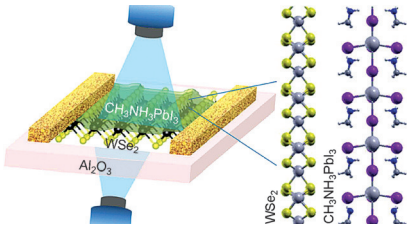

Heterogeneous Catalysis

A synergistic catalyst of $Cu_xCo_{1-x}O$ nanoparticles on graphene oxide achieves a TOF value of 70.0 (H_2) mol/(Cat-metal) mol·min for the hydrolysis of ammonia–borane, which is the highest value ever reported for noble-metal-free catalysts. The hydrolysis mechanism was also studied by in situ XAS experiments for the first time.

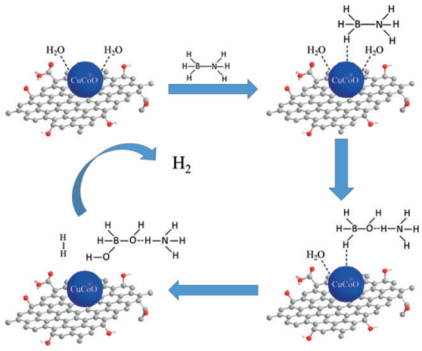

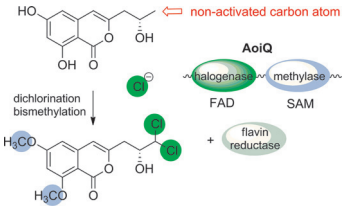

Multitasking enzyme: Prompted by the discovery of unusual halogenated polyketides, so-called dichlorodiaporthins, in cultures of a fungus widely used for food fermentation (*Aspergillus oryzae*), a novel biocatalyst (AoiQ) was identified that not only mediates a phenolic bismethylation but also introduces a geminal dichloro moiety at an unactivated aliphatic carbon atom.

Enzymatic Halogenation

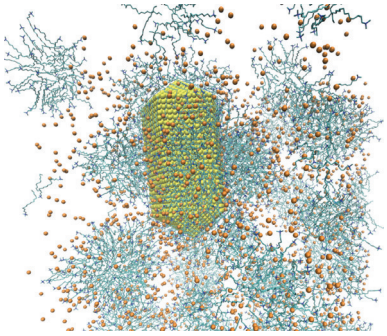

Molecular dynamics simulations were applied to shed light on the growth mechanism of gold nanorods and to determine the role of surfactants and ions in this process. The symmetry of the nanoseeds is broken early on as the surfactant layer preferentially covers the (100) and (110) facets. This anisotropic surfactant layer promotes anisotropic growth, with the less protected tips growing faster.

Crystal Growth

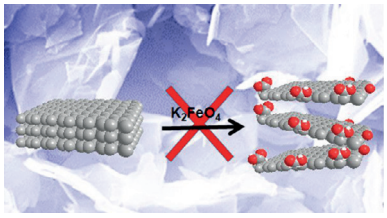

Ferrate-ing around: The oxidation of graphite by ferrate(VI) is impossible owing to its fast decomposition in an acidic environment. Any oxidation occurring when using commercial potassium ferrate(VI) is caused by impurities.

Graphene Oxide

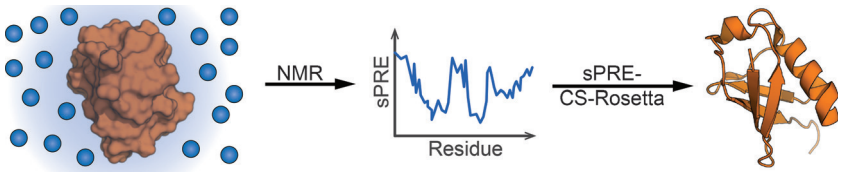

Protein structures can be predicted by using surface accessibility data from NMR paramagnetic relaxation enhancements by a soluble paramagnetic compound (sPRE). This method exploits the distance-to-surface information encoded in the sPRE data in the chemical shift-based CS-Rosetta de novo structure prediction framework to generate reliable structural models.

Structural Biology

Polymerization

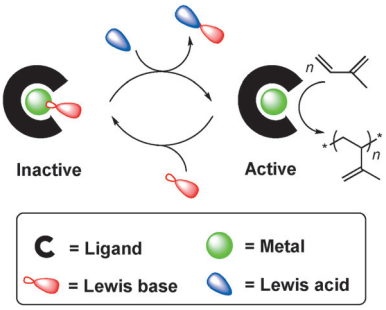

Going round in circles: Temporally and stereocontrolled coordination polymerization was achieved by switching the activity of a Lewis acidic metal catalyst by alternating addition of a Lewis base and a Lewis acid. The switching process was rapid, quantitative, and could be repeated multiple times; not only the catalytic activity but also the selectivity of the polymerization were controlled.

Supramolecular Chemistry

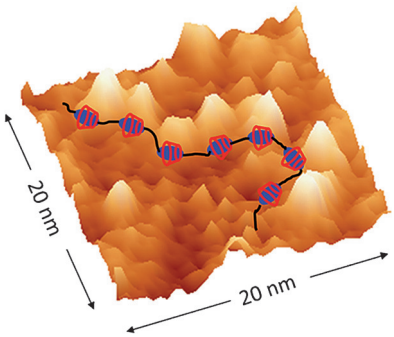

A molecular necklace of polypseudorotaxanes was prepared by threading β-cyclodextrins (β-CD; see picture, red) onto biodegradable and thermoresponsive polyurethanes derived from bile acids. The β-CD rings slide onto the poly(ethylene glycol) segments (black) and selectively recognize the bile acid units (blue) of the polyurethane chains. This bio-compound-derived molecular necklace can be visualized by the scanning tunneling microscopy.

Organic Semiconductors

Temporary solubilization: The Lewis acidity of boron-containing polycyclic aromatic hydrocarbons (PAHs) offers an opportunity to increase their inherently poor solubility by the formation of dynamic Lewis acid–base complexes with simple pyridine derivatives. Spin-coating of 1 wt% pyridine-containing solutions of these PAHs, followed by thermal annealing, affords thin-film transistors that show typical p-type characteristics.

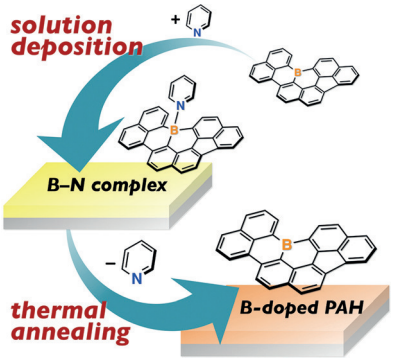

Emission Control

Selective catalytic reduction of NO with ammonia on vanadium goes Lewis: A combination of time-resolved diffuse reflectance IR spectroscopy (DRIFTS) and visible spectroscopy (DR-Vis) with a modulated excitation approach, provided unambiguous evidence for the participation of Lewis acid sites in the selective catalytic reduction of NO with NH_3 over V_2O_5-WO_3-TiO_2 catalysts.

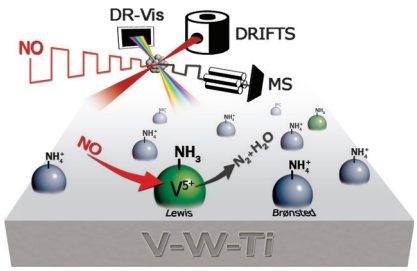

Linear alignment: Model iron nitrosyl complexes have been well-studied due to their biological significance and interesting underlying electronic structures. However, species with high Enemark–Feltham numbers (8–10) remain rare. An unusual redox series of $\{FeNO\}^{8-10}$ complexes supported by a tris(phosphine)borane maintains a linear Fe-N-O angle throughout the series; the reasons for this atypical behavior have been investigated spectroscopically.

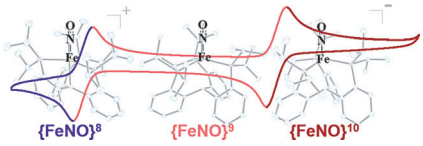

Iron Nitrosyl Complexes

Easy as 0, 1, 2: A series of ruthenium complexes with oxidation states $n = 0$, $+1$, and $+2$ is described with $[Ru(tropPPh_2)_2]^n$ of identical chemical composition but remarkably different structure. In the Ru^I complex, the single unpaired electron is mainly localized on the metal center.

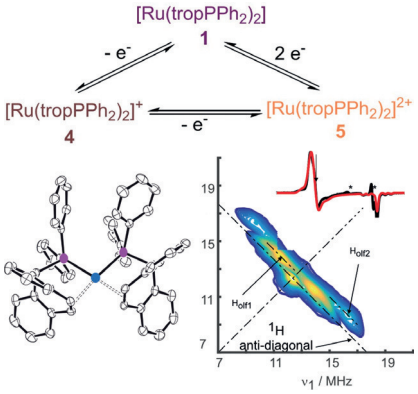

Ruthenium Complexes

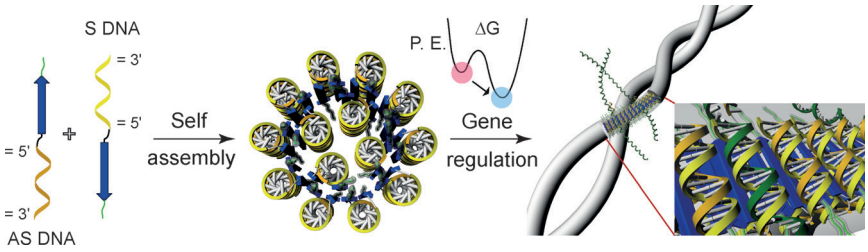

DNA and peptides play ball: Orthogonal self-assembly modes of the β-sheet peptide and DNA were covalently combined to construct ΔG programmable supramolecular nanostructures. The covalent constraint enables the formation of well-defined assemblies capable of regulating gene expression with low cytotoxicity. P.E. = potential energy.

Self-Assembly

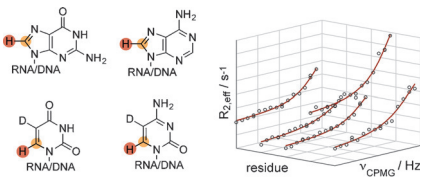

Excited protons: Nucleotide chemistry and state of the art NMR methods are combined to probe excited states of RNA and DNA via proton relaxation dispersion experiments. The approach will be very useful for the elucidation of high-resolution excited state structures of nucleic acids.

NMR Spectroscopy

Gene Delivery

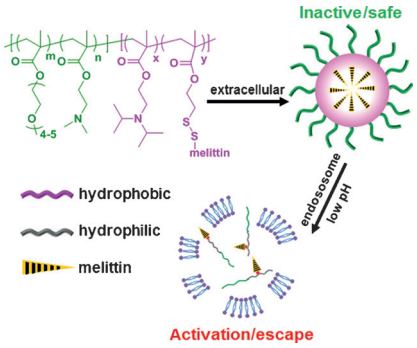

A virus-inspired polymer is reported as an effective gene transfer vehicle. The polymer, called VIPER (virus-inspired polymer for endosomal release), is composed of a polycation block for nucleic acids condensation and a pH-sensitive block for acid-triggered display of a lytic peptide to promote trafficking to the cell cytosol both in vitro and in vivo.

Glycobiology

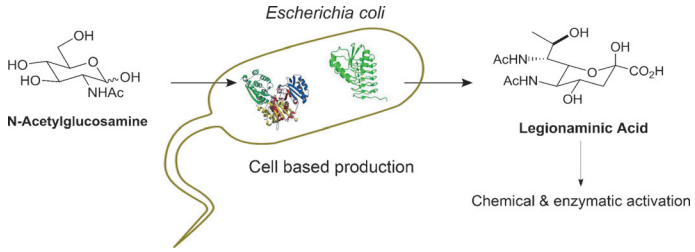

A cell-based metabolic engineering strategy for the production of the complex carbohydrate legionaminic acid ($Leg5,7Ac_2$) was achieved. Metabolic modules from three different microbial sources were used to generate a de novo biosynthetic route to access $Leg5,7Ac_2$. Chemoenzymatic and chemical activation of $Leg5,7Ac_2$ is also presented.

Heterogeneous Catalysis

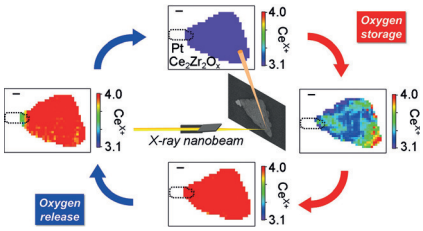

Visualizing heterogeneous reaction modes: Oxygen diffusion in individual Pt/$Ce_2Zr_2O_x$ particles in a three-way conversion catalyst was imaged by scanning nano-XAFS. Non-uniform oxygen diffusion modes and active parts were successfully visualized for oxygen storage and release. Scale bar: 500 nm.

Cascade Reactions

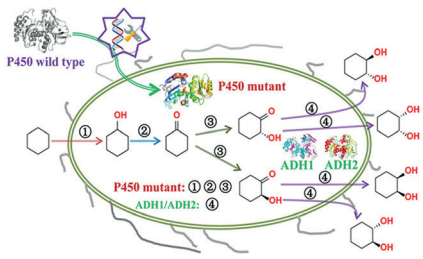

Four steps in one pot: *E. coli* cells harboring P450-BM3 mutants and appropriate alcohol dehydrogenases were obtained by directed evolution. Such cells enable one-pot cascade reactions of cyclohexane with selective formation of all three stereoisomeric cyclohexane-1,2-diols.

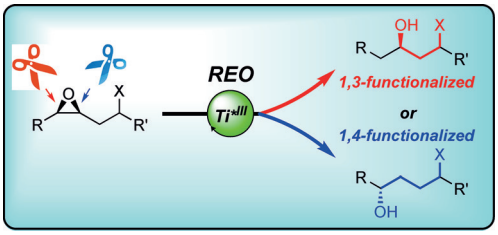

Like enantio-scissors: Highly regioselective bond-scission with enantiomerically pure or racemic β-substituted epoxides is accomplished by enantiomerically pure titanocenes (see scheme; REO = regiodevergent epoxide opening). Substrate synthesis is modular and the products, 1,3- or 1,4-functionalized alcohols, are valuable intermediates for natural product synthesis and for the preparation of biologically active substances.

Enantioselective Synthesis

A glucose conjugate of the anti-inflammatory natural product triptolide, glutriptolide, was developed that selectively targets tumor cells overexpressing glucose transporters. Glutriptolide demonstrated significantly higher cytotoxicity against tumor cells than against normal cells and also benefitted from improved water solubility compared with triptolide.

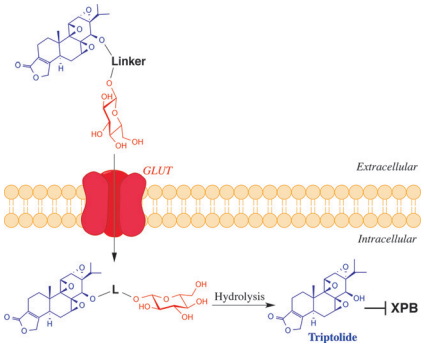

Antitumor Agents

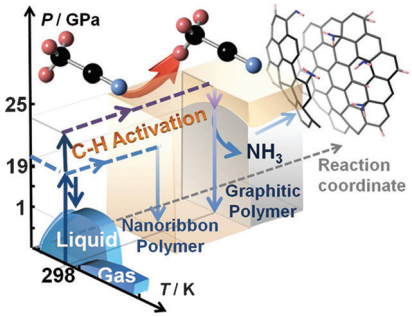

Under high pressure, the C≡N bond of acetonitrile is expected to polymerize into conjugated C=N bonds. It is however shown that when compressing CH_3CN at 25 GPa, a hydrogen atom transfers along the $-H_2C-H\cdots NC-$ hydrogen bond, which triggers the polymerization to form a dimer, 1D chain, and 2D nanoribbon. Finally, it converts into a graphitic polymer accompanied by the release of ammonia.

High-Pressure Polymerization

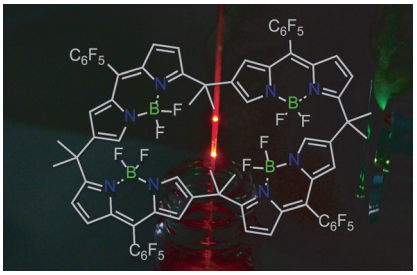

2C; confusion and cyclization: Circularly orientated BODIPY-based macrocycles were synthesized based on multiply N-confused calix[*n*]phyrin (*n* = 4, 6, 8) derivatives. These novel BODIPYmers exhibit unique size-dependent photophysical properties.

Calixphyrin Complexes

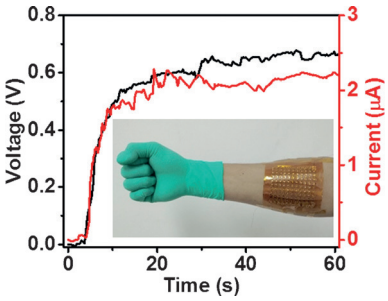

A flexible and wearable integrated thermocell based on gel electrolytes was designed. Utilizing body heat, an output voltage of almost 1 V was achieved, offering a new train of thought for self-powered wearable systems that harvest low-grade waste heat.

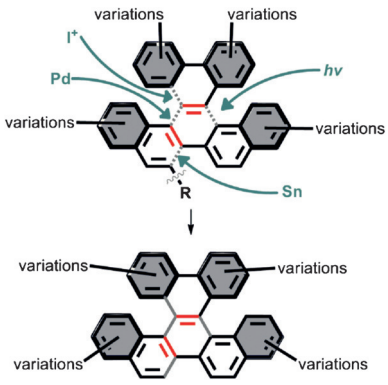

A new approach to fused helicenes is reported, in which varied substituents are readily incorporated in the extended aromatic frame. From an alkynyl precursor, the final helical compounds are obtained in a two-step process, in which the final C—C bond is photochemically forged by coupling cyclization and dehydroiodination. The distortion of the π-system from planarity leads to unusual packing in the solid state.

Glowing zippers: Luminescent Eu^{III} coordination polymers were successfully fabricated by introducing a densely packed coordination zipper structure. These hydrogen-bonded coordination polymers have a high energy transfer efficiency of 80% and thermal stability up to 320 °C.

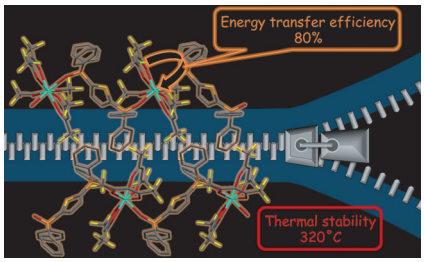

A technical dream-coat: Ten common metal oxide nanoparticles were classified into three groups based on their interaction with two related liposomes. Enveloping a magnetic iron oxide core with a lipid shell facilitates bioconjugation, biocompatibility, and delivery.

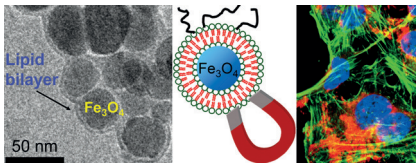

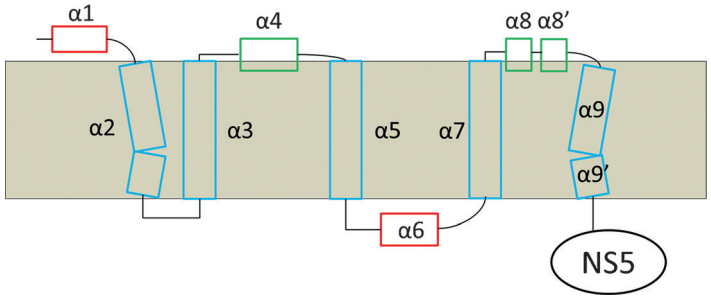

On top of the topology: The membrane topology of the dengue virus 3 NS4B was determined based on secondary structures, and various NMR spectroscopy techniques including paramagnetic relaxation enhancement (PRE) and H–D exchange experiments. This study provides atomic-level information for an important drug target to control flavivirus infections.

Protein Structure

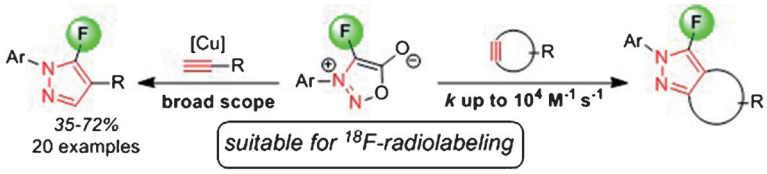

Fast and fluorious: Fluorosydnones are extremely reactive towards copper-catalyzed cycloaddition reactions with terminal alkynes and copper-free reactions with cycloalkynes. These highly reactive clickable reagents were prepared by electrophilic fluorination of sydnone Pd^{II} precursors in the presence of Selectfluor.

Click Chemistry

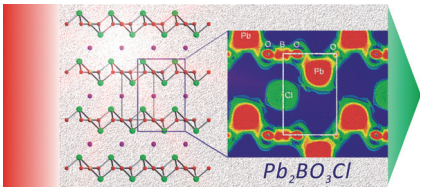

Polar, non-centrosymmetric Pb_2BO_3Cl consists of cationic $[Pb_2(BO_3)]^+$ honeycomb layers and Cl^- anions. The title compound is phase-matchable (type I) and exhibits a remarkably strong second harmonic generation (SHG) response, which is approximately nine times stronger than that of potassium dihydrogen phosphate.

Second Harmonic Generation

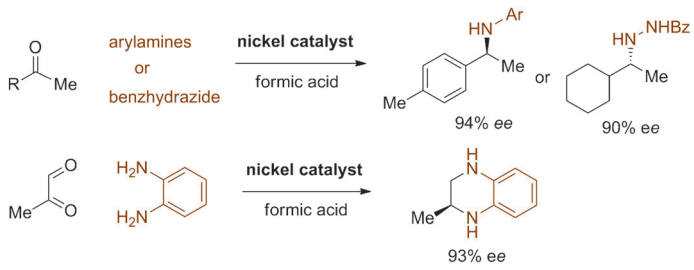

Reducing costs: Reductive amination of ketones with both arylamines and benzhydrazide was realized in the presence of catalysts based on nickel rather than expensive noble metals. Formic acid was used as a safe and cheap surrogate for high-pressure hydrogen gas.

Asymmetric Hydrogenation

Helical Structures

The nucleating effect of the template is subtly influenced by substitution tuning on the side-chain-end tether. Unlike most nucleating strategies, the N-terminal NH_2 is preserved, thus enabling further modification. Peptidomimetic estrogen receptor modulators constructed with this method show improved therapeutic properties. Dap = 2,3-diaminopropionic acid.

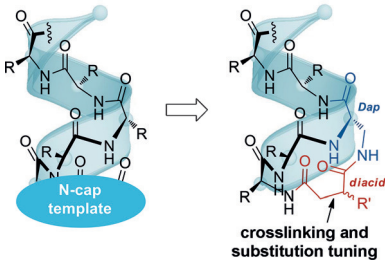

Noncovalent Interactions

Entropy vs. enthalpy: Self-assembly of PBI **1** in water is governed by two major contributions with inverse thermodynamic parameters, the enthalpically driven π–π stacking between the hydrophobic π-cores and the dominant entropic release of water molecules from the hydrophilic moiety. The thermodynamic behavior can be inverted by addition of an organic cosolvent.

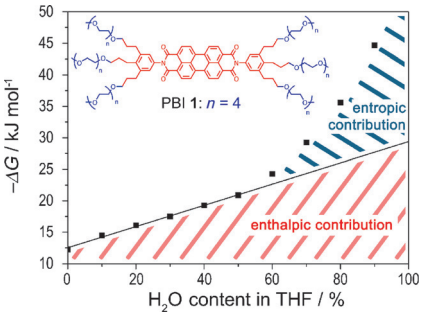

MOF–Polymer Composites

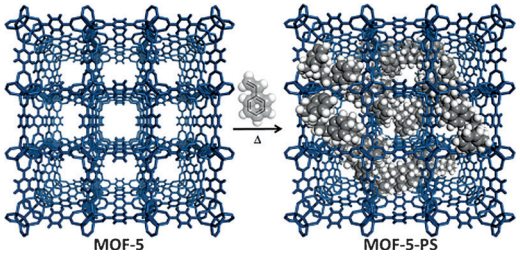

MOFs packed with polystyrene: An unprecedented mode of reactivity of one of the best studied metal–organic frameworks, MOF-5, offers a powerful approach to polymer-hybridized porous solids. A MOF-5-polystyrene (MOF-5-PS) composite was directly produced from the monomer styrene. In the MOF-5-PS composites, polystyrene is grafted and uniformly distributed throughout, which leads to enhanced hydrolytic stability and unique guest adsorption.

Domino Reactions

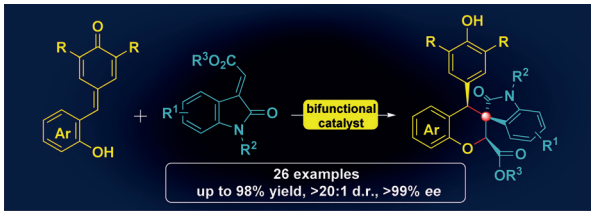

Hydroxy-substituted *para*-quinone methides were successfully used in an asymmetric organocatalytic oxa-Michael/1,6-addition domino reaction. In the presence of a bifunctional thiourea organocatalyst, this reaction afforded a wide range of 4-aryl-substituted chromans with an oxindole scaffold and three contiguous stereocenters in high yields and stereoselectivities.

Supporting information is available on www.angewandte.org (see article for access details).

A video clip is available as Supporting Information on www.angewandte.org (see article for access details).

This article is available online free of charge (Open Access).

This article is accompanied by a cover picture (front or back cover, and inside or outside).

The Very Important Papers, marked VIP, have been rated unanimously as very important by the referees.

The Hot Papers are articles that the Editors have chosen on the basis of the referee reports to be of particular importance for an intensely studied area of research.

Angewandte Corrigendum

Figure 2 in this Communication is accidentally identical with the bottom panels of Figure 1, whereas the legend corresponds to the original diagrams planned to be shown there. The corrected Figure 2 is displayed below. The authors apologize for this oversight.

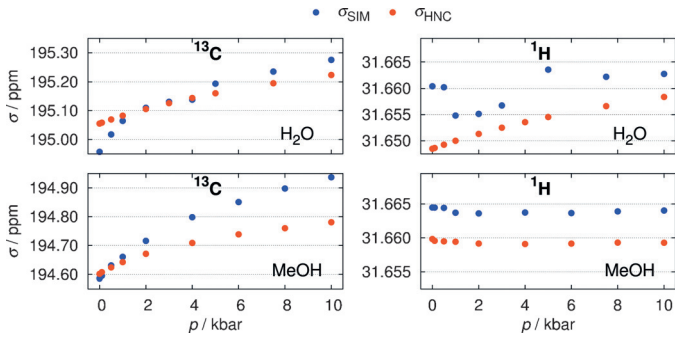

Figure 2. Pressure-dependent shielding constants of the DSS anion from GIAO/EC-RISM/B3LYP/6-31+G(d,p) calculations in water (top) and methanol (bottom) for ^{13}C (left) and ^{1}H (right) of the DSS methyl groups with χ taken from MD (orange) and HNC (blue). Data reflect arithmetic averages over equivalent nuclei.

The Chemical Shift Baseline for High-Pressure NMR Spectra of Proteins

R. Frach, P. Kibies, S. Böttcher, T. Pongratz, S. Strohfeldt, S. Kurrmann, J. Koehler, M. Hofmann, W. Kremer, H. R. Kalbitzer, O. Reiser, D. Horinek, S. M. Kast* _____ **8757–8760**

Angew. Chem. Int. Ed. **2016**, *55*

DOI: 10.1002/anie.201602054

